Nucleic Acids Research, 1998, Vol. 26, No. 2 655–661

Three-dimensional structure of the yeast ribosome

Adriana Verschoor[1,*], Jonathan R. Warner[3], Suman Srivastava[1], Robert A. Grassucci[1] and Joachim Frank[1,2]

[1]Wadsworth Center, New York State Department of Health, Empire State Plaza, PO Box 509, Albany, NY 12201-0509, USA, [2]Department of Biomedical Sciences, State University of New York at Albany, Empire State Plaza, Albany, NY 12201-0509, USA and [3]Department of Cell Biology, Albert Einstein College of Medicine, 1300 Morris Park Avenue, The Bronx, NY 10461, USA

Received July 16, 1997; Revised and Accepted November 12, 1997

ABSTRACT

The 80S ribosome from *Saccharomyces cerevisiae* has been reconstructed from cryo electron micrographs to a resolution of 35 Å. It is strikingly similar to the 70S ribosome from *Escherichia coli*, while displaying the characteristic eukaryotic features familiar from reconstructions of ribosomes from higher eukaryotes. Aside from the elaboration of a number of peripherally located features on the two subunits and greater overall size, the largest difference between the yeast and *E.coli* ribosomes is in a mass increase on one side of the large (60S) subunit. It thus appears more elliptical than the characteristically globular 50S subunit from *E.coli*. The interior of the 60S subunit reveals a variable diameter tunnel spanning the subunit between the interface canyon and a site on the lower back of the subunit, presumably the exit site through which the nascent polypeptide chain emerges from the ribosome.

INTRODUCTION

The recent completion of the sequence of the genome of *Saccharomyces cerevisiae* (1), as well as determination of the entire set of mammalian ribosomal proteins (2; I.G.Wool, personal communication), has permitted us a look at the entire complement of the yeast ribosome. The yeast ribosome is composed of two subunits. The 60S subunit contains three RNA molecules: 25S RNA of 3392 nt, hydrogen bonded to the 5.8S RNA of 158 nt and associated with the 5S RNA of 121 nt. There are 42 proteins in the large subunit, plus two copies each of two acidic exchangeable proteins. Altogether there are 3671 nt and 7235 amino acids in the 60S subunit, giving it a ratio of ~61% RNA to 39% protein. The 40S subunit has a single RNA of 1798 nt and 32 proteins with a total of 4749 amino acids, giving it a ratio of 54% RNA to 46% protein. All identified yeast ribosomal proteins are represented by homologous proteins in the mammalian ribosome, which has a single protein, L28, that appears not to be present in yeast. It will be interesting to learn whether L28 is present in ribosomes of higher plants as well as those of intermediate species such as *Caenorhabditis elegans* and *Drosophila*. Mammalian ribosomes differ from fungal ribosomes mainly in the size of the large RNA of the large subunit: mammalian 28S RNAs may exceed 5000 nt in length, compared with roughly 3400 nt for the fungal (as well as higher plant) 25S RNAs.

Thus, except for the mammalian ribosome having longer RNA molecules and slightly larger proteins, there is a remarkable conservation of the elements of this master machine of translation.

Following our study of the three-dimensional (3D) structure of the wheatgerm ribosome (3) we felt it valuable to examine in detail the structure of another eukaryotic ribosome, one that provides the opportunity of exploration using genetic methods.

MATERIALS AND METHODS

Ribosomes were isolated from *S.cerevisiae* strain W303 (4) essentially as described (5). Briefly, the cells were collected by centrifugation, washed in water and resuspended in TMN (50 mM Tris–acetate, pH 7.4, 50 mM NH_4Cl, 12 mM $MgC1_2$, 1 mM DTT) and broken by vigorous agitation with glass beads. After two cycles of low speed centrifugation the supernatant was centrifuged for 3 h at 50 000 r.p.m. through a cushion of TMN containing 5% $NH_4(SO_4)_2$ and 10% sucrose, in order to separate the ribosomes from any soluble proteins and to strip off any loosely bound proteins. Subunits derived from ribosomes prepared in a nearly identical way have proved to have activity in several protein synthesis assays (6,7). This was also the method used to prepare the ribosomes used in the definition of the set of ribosomal proteins present in yeast (5).

Grids were prepared for cryo microscopy according to standardized methods in our laboratory following Wagenknecht *et al.* (8) and Dubochet *et al.* (9). Micrographs were recorded using low dose protocols in a Philips EM420 at a magnification of 38 000×; the resulting pixel size was 5.26 Å.

Twelve micrographs at 0°, 35° and 50° tilts were analyzed. Analysis was of 7470 projections with a projection matching scheme (10). For this an initial reference was a low pass filtered structure obtained previously (3) for the wheatgerm ribosome. This wheatgerm structure had been obtained from tilt pair data according to a random conical reconstruction scheme, with the missing cone information filled in by projection onto convex sets (POCS; see for example 11). After the first iteration of

*To whom correspondence should be addressed. Tel: +1 518 486 4909; Fax: +1 518 474 8590; Email: adri@orkney.ph.albany.edu

reconstruction for the initial yeast data set, however, the reference was successively replaced by the current highest quality yeast ribosome reconstruction.

Initially 2348 projections from four 0° micrographs were processed, but multivariate statistical analysis and hierarchical ascendent classification revealed the paucity of certain view ranges, indicating that the 80S ribosome could not be reconstructed without tilt data, in contrast to the *E.coli* 70S ribosome. Subsequently tilt micrographs were added two by two. These data sets were processed independently, after incorporation of the original tilts allowed adequate infilling of the angular space. Analysis of subsequent data increments was based on the reference derived from this stage, but the projection sets used were completely independent. This allowed the quality and completeness of the 35° and 50° tilt sets to be gauged. Finally, all data sets were pooled and the SIRT back-projection algorithm (12) was iterated until the results stabilized.

The full data set was highly anisotropic in nature, with an extreme over-representation of only two or three preferred views, in striking contrast to the *E.coli* 70S ribosome, which assumes a sufficient number of orientations that tilt micrographs are not needed. For the eukaryotic ribosome it was found necessary to collect 35° and 50° tilt images to fill in the areas of missing information in Fourier space. The main consequence, beyond the necessity of recording tilt data, was that a large number of iterations of the SIRT back-projection algorithm were needed to overcome the weighting bias caused by the preponderance of $\phi = 0$, $\theta = 0$ projections. For the final reconstruction 200 iterations of the SIRT algorithm were used. The resultant structure was examined and compared with existing structures for the eubacterial and eukaryotic ribosomes through surface representations. The structure was further analyzed using the AVS (Advanced Visual Systems Inc., Waltham, MA) and O (13) graphics softwares.

RESULTS

The 80S ribosome from *S.cerevisiae* has been reconstructed from 7470 individual ribosome images to a resolution of 35 Å according to the Fourier Shell Criterion measure, using a critical value of 0.5 (14), corresponding to a signal-to-noise ratio of ~2 (15). This value closely agreed with the value obtained by the 45° phase residual criterion used in previous studies. Low pass filtration to 35 Å and, for correction of the transfer function, Wiener filtration were then applied.

Morphology of the yeast ribosome

The yeast ribosome is a bipartite structure that varies from roughly equidimensional to somewhat elongate depending on viewing angle (Fig. 1). In the orientation shown in Figure 1A the two subunits are seen side by side, 40S subunit on the left and 60S subunit on the right, with their 'heads' at the top. In this view the height of the ribosome is ~254 Å, the width ~278 Å and the thickness ~267 Å. These height and width dimensions are 11–14% smaller than those calculated for the ribosome from a higher eukaryote, wheatgerm (3), but greater than those for the 70S *E.coli* ribosome (Fig. 1). That the thickness dimension is significantly greater for the yeast structure than for wheatgerm could be a result of experimental differences (see Discussion).

At the threshold used for surface representation (e.g. Fig. 1) the volume of the yeast ribosome reconstruction is calculated to be ~4.34×10^6 Å^3. This figure may be compared with a volume of 3.4×10^6 Å^3 for the *E.coli* ribosome (at 25 Å resolution) visualized at an analogous threshold. These volume estimates are significantly higher than those obtained from simple summation of the molecular masses of the rRNA and ribosomal proteins: 2.6×10^6 Å^3 for *E.coli* (16) and 3.41×10^6 Å^3 for yeast [calculated from mass data given in (17) and the RNA/protein ratios given above; see Introduction]. The choice of threshold relative to the calculated theoretical mass of the components was made to enable direct comparison with the published *E.coli* structures (18–19). However, the volume estimate that corresponds to a given threshold is extremely sensitive to several factors, among which is uncertainty in the electron microscopic magnification (16). As discussed by Frank and Agrawal (20), the appropriate choice of threshold should rather be based on innate criteria such as contiguity of the mass.

The two subunits of the yeast ribosome are clearly separated, as can be seen in side-by-side views (Fig. 1E and J). In fact, a plane can be interposed (Fig. 1K) to cut the subunits apart, bisecting two connecting bridges. The larger bridge links the mid portions of the subunits, the interface aspect of the 40S subunit platform structure and the flattish interface surface of the 60S subunit directly below the interface canyon (see Fig. 2C). The morphology of this bridge (Fig. 1A and J) agrees well with that described for the wheatgerm ribosome (3). A second, somewhat smaller diameter bridge links the subunit bases (Fig. 1E and J). Unlike the main central bridge, this bridge can be pinched off by moderately increasing the threshold used for visualization.

The 'eukaryotic elaborations' described for the wheatgerm ribosome (3) are clearly seen in the yeast ribosome, notably the elongate beak and angled ear on the head of the 40S subunit, the knob-like back lobes superimposed on the cup-shaped platform structure and the feet comprising the broad base of the 40S structure. Two horizontally tending structures related to the organization of the stalk base ridge of the 60S subunit (Fig. 1G and H) are strongly developed and give a forked appearance to this side of the large subunit.

The most striking point in the comparison in Figure 1 is the extent to which the yeast ribosome resembles the *E.coli* ribosome, except for an evident expansion of the former along one axis. The 60S large subunit appears as though stretched along a lateral axis to a more ellipsoidal form than the compact 50S subunit shape. The yeast 40S subunit appears as if certain vestigial protuberances discernible in the *E.coli* 30S subunit have developed into the characteristically extended eukaryotic features (beak, feet). Beyond this impression of localized expansions in the yeast ribosome, however, the resemblance to the *E.coli* ribosome is quite marked.

Large subunit tunnel

Although a number of low density internal features can be recognized in the yeast ribosome; features continuous between the interface surface and the back of the large subunit are of particular interest. These represent candidates for the postulated tunnel through which the nascent polypeptide chain exits the ribosome (see Discussion). In the following we make use of surface representations (Fig. 2A and B) and a cutaway stereo representation (Fig. 3) to investigate two low density features that issue from a deep depression in the IC and traverse the subunit to debouche at sites on its back. The lower tunnel feature is strikingly goblet-shaped (Fig. 3), tapering rapidly to a narrow stem that ends as a small hole on the lower back of the subunit (Fig. 2B). The upper tunnel feature is broader and less variable in

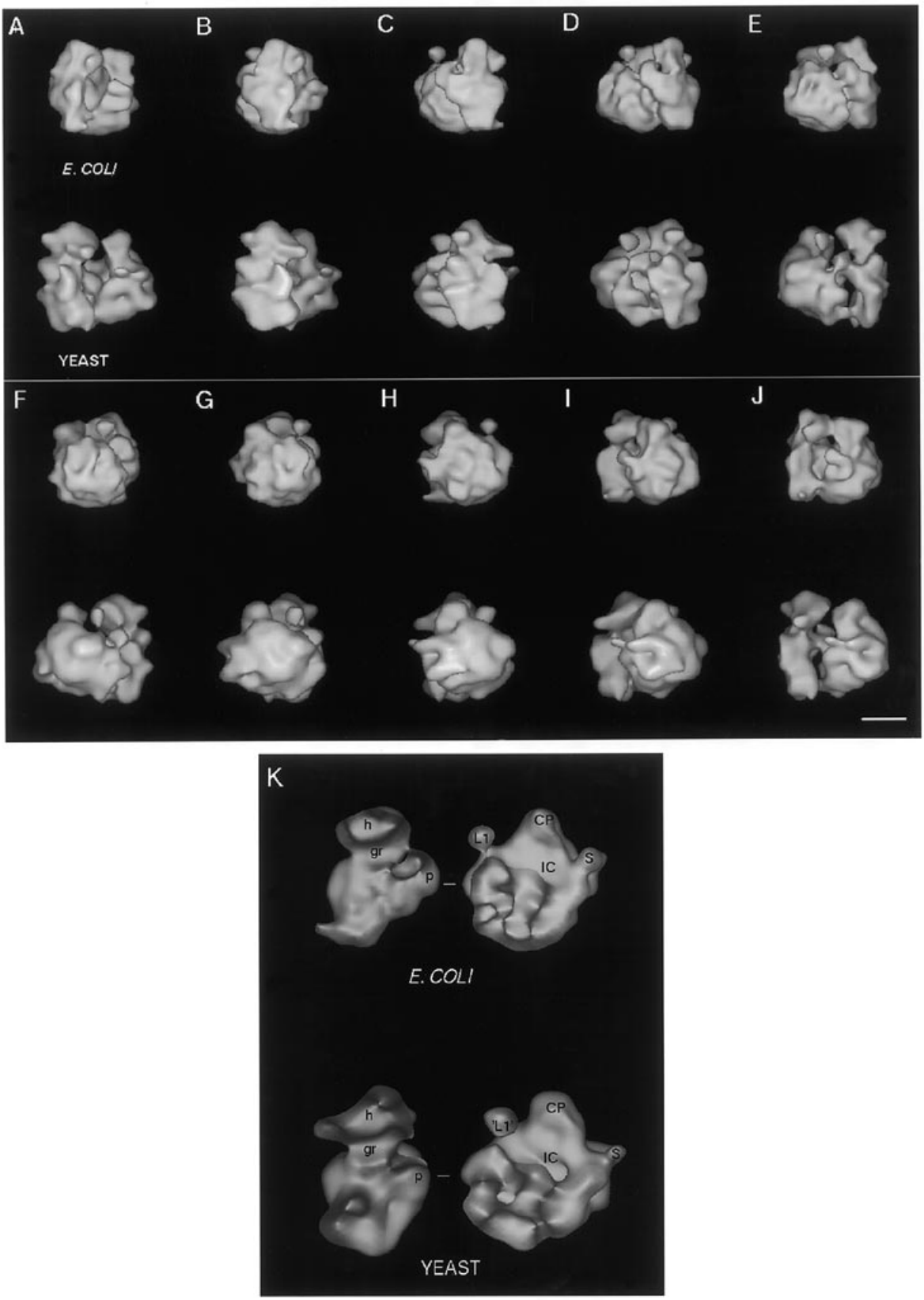

Figure 1. Comparison of ribosome structures: *E.coli* 70S (upper row in each panel, structure from 18,19) and yeast 80S (lower row in each panel) ribosomes, both limited to 35 Å resolution. (**A–J**) Rotational series, with a rotational increment around the vertical axis of 36°. Scale bar 100 Å. (**K**) Exploded views of *E.coli* and yeast ribosomes, showing close correspondence of features of interface surfaces of ribosomal subunits, most notably the interface canyon (IC). CP, central protuberance; S, stalk; L1 or 'L1', L1 or L1 analog arm; h, head; g, neck groove; p, platform. Note that the lower right portion of the small subunit and the lower left portion of the large subunit are surfaces where the sectioning plane has cut a mass that is merged between the two subunits at this resolution.

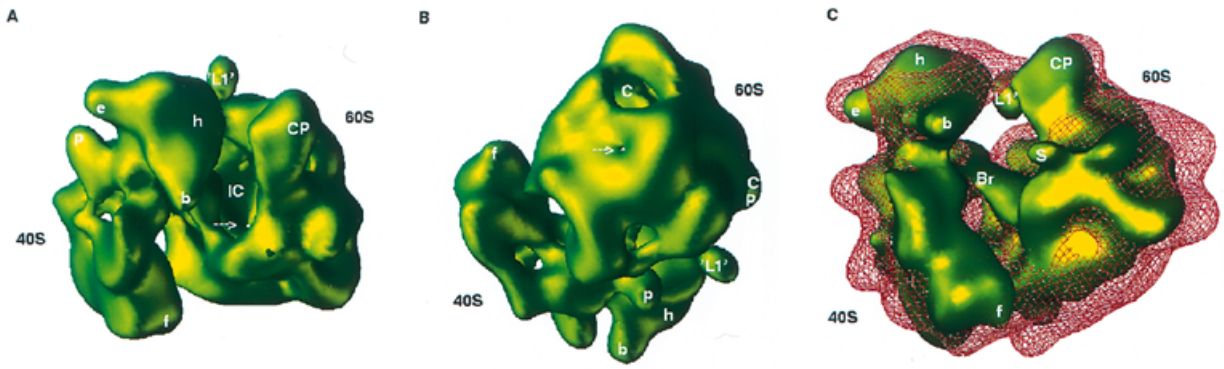

Figure 2. Structural features of the yeast ribosome. (**A** and **B**) Surface low density features of the large subunit; (**C**) comparison with cytoplasmic ribosome structure from a higher eukaryote. Labels of features as in the legend to Figure 1K; f, feet; b, beak; e, ear; Br, main bridge between subunits. (A and B) Two views of the yeast ribosome (at a slightly elevated threshold), related by a rotation of 180° around the horizontal axis in the image, showing the two ends of a small but clearly resolved low density feature through the large subunit, as seen from (A) the interface side of the 60S subunit and (B) the back or membrane facing side of the 60S subunit. In (A) the hole (marked by an arrow) into the interface surface of the 60S subunit is seen in the deepest portion of the IC. In (B) a rotation of 180° around a horizontal axis has been applied, to reveal the opposite end of the low density feature seen in (A). An arrow indicates the small hole that represents the putative exit tunnel. The extremely large cavity (C) above the hole is the site of emergence of the large diameter upper tunnel. (C) Comparison of yeast ribosome structure with wheatgerm ribosome structure. Yeast structure is shown as a green solid surface; the envelope of the wheatgerm structure (3) is shown as a red net. Structures are shown aligned in the side by side orientation. The greater height and width of the wheatgerm structure but greater (front-to-back) thickness of the yeast structure can be seen. All of the protruding features, such as the back lobes of the 40S subunit, in the wheat structure have counterparts in the yeast structure. However, the latter is markedly more compact and globular.

diameter and it is situated more to the stalkward side of the subunit, i.e. in a plane closer to the viewer in Figure 3. This latter broad tunnel is sectioned by the clipping plane in this figure, whereas the lower tunnel is further from the viewer (closer to the midline of the subunit), behind the sectioning plane. The broad tunnel ends as a very large cavity in the mid back of the subunit (Fig. 2B).

Comparison of large subunits from the eubacterium *E.coli* and the eukaryote *S.cerevisiae* (18,21; Malhotra *et al*., submitted for publication; Verschoor *et al*., work in progress) reveals that the lower tunnel is a highly conserved morphological feature and thus merits particular attention. It provides a strikingly direct conduit between the interface and back aspects of the subunit. As can be seen from Figure 3, it appears to represent the shortest possible connection, in geometric terms, between the interface and cytoplasmic surfaces of the subunit or between the classical translational and exit domains.

DISCUSSION

Comparison with the *E.coli* ribosome

Overall the yeast ribosome is strikingly similar to the *E.coli* ribosome at a comparable resolution (Fig. 1). It is somewhat larger and more elaborated morphologically, but the degree of agreement in the shapes as the structures are rotated is remarkable. For many features the difference is a matter of degree; generally the *E.coli* ribosome has a counterpart feature to the yeast, but it is less strongly expressed. Particularly notable is the small subunit beak.

In most of the views shown in Figure 1 (except for panels B, F and G) the yeast ribosome strongly resembles the 70S *E.coli* ribosome. The principal difference is in the shape of the small subunit. In views where the small subunit is seen in lateral view (e.g. Fig. 1B and C) the characteristically eubacterial versus eukaryotic features of this subunit allow the two ribosomes to be identified unambiguously. Although the *E.coli* 30S subunit is now recognized as having a broad nose-like front portion to the head, with a very marked bend to the tip, the beak or bill of the eukaryotic subunit differs in its greater degree of extension. Likewise, the crest described for the eukaryote (22–24) remains a key identification element, even subsequent to recognition (e.g. Fig. 4E and F in 18) of a comb- or wattle-like feature trailing down the back of the neck of the *E.coli* subunit (see 19, fig. 4A and B). The eukaryotic crest is a feature of the head *per se* and has not been observed to lie along the neck.

The features that do differ tend to be peripherally located. In the 40S subunit we see no trace of the spur feature noted for the *E.coli* subunit (10,18–19), but rather a broad square base. The classical eukaryotic feet (3,25) are recognizable, though not highly elaborated in this yeast structure; a small conical front foot can be discerned (Fig. 1A and H–J). Also, the platform, while now recognized as a well-developed feature in eukaryotes (cf. 3), is nevertheless not as extended in the yeast structure as in the *E.coli* structure (Fig. 1D).

Recent *E.coli* ribosome reconstructions (16,18–19) have revealed some surprising features, which in fact serve to increase the resemblance to the 40S subunit, with all of its so-called eukaryotic additions. Among the most marked similarities are comparable morphologies of the head, platform and the groove that constitutes the interface surface of the small subunit neck. Exploded views (Fig. 1K) reveal virtually identical morphologies in this key region of the translational domain (see below).

For rotations in which there is a difference in overall form between the two ribosome structures this difference is usually attributable to the larger and more ellipsoidal form of the 60S subunit, as compared with the globular 50S subunit of the *E.coli* ribosome. The 60S subunit is characterized by its obliquity (relative to an axis in which the central protuberance is directed vertically), with a trapezoidal rather than circular outline. On the side of the ribosome bearing the so-called L1 analog arm the base

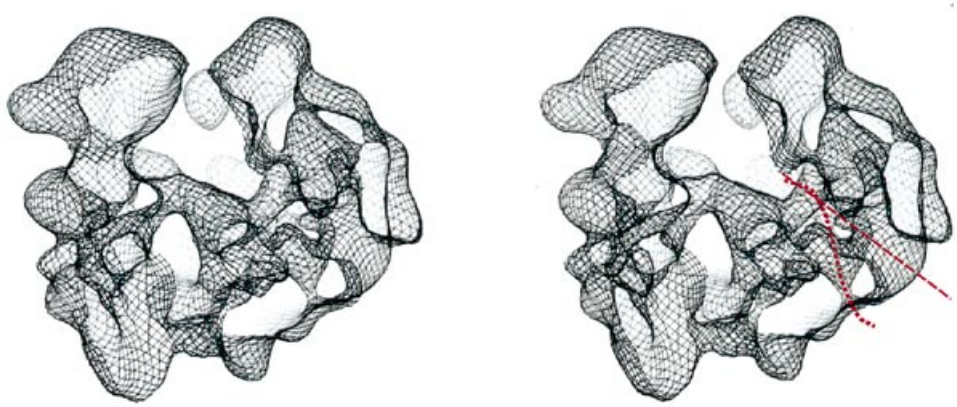

Figure 3. Low density internal features of the 60S subunit. Stereo representation of the yeast ribosome in a side by side view (cf. Fig. 2C for identification of features in the same view), with a portion of the structure in front cut away. This allows recognition of two of the principal low density features, or presumptive tunnels, that traverse the 60S subunit between the IC (upper left ends of dashed lines) and the mid and lower back (lower right ends of dashed lines) of the subunit. The straight dashed line indicates the axis of the very large tubular feature that is bisected by the clipping plane in this representation. It traverses the subunit in a plane markedly to the stalkward side of the midline of the subunit (i.e. the top-to-bottom axis when the subunit is in the crown orientation, with the CP at the top). Although it is roughly linear, it has one notable branch (not shown) that runs nearly vertically to a point behind the CP. The curved line indicates a route through the more variable tunnel, from the IC into a goblet-shaped wide segment that then rapidly tapers and emerges via a small hole in the lower back of the subunit. The goblet portion has a ruffled lip but is completely open to the IC entry region. This variable tunnel runs more or less parallel to the midline of the subunit. It is clearly homologous to the tunnel seen in the *E.coli* ribosome (18,19; Penczek *et al.*, submitted for publication) and recent ligand studies on yeast ribosomes (see text) implicate it in co-translational movement of the nascent polypeptide chain. Note that the resolution limitation has been relaxed slightly in this representation, to allow optimal delineation of the internal features. However, the same morphology is clear at the reproducible resolution of 35 Å.

of the subunit has a strongly diagonal facet that seems to represent a local concentration of ribonucleoprotein not seen in the 50S subunit.

While these external aspects of the large subunit show what appear to be evolution-related mass increases, the interface aspect strikingly does not. From the interface side exploded views of the *E.coli* and yeast ribosomes (Fig. 1K) show the 60S subunit to be highly similar to the 50S subunit. The central IC feature is virtually identical in form and trend in the two structures and the three peripheral protuberances characteristic of the classical 'crown' orientation of the subunit show an excellent match. It may well be significant that in terms of features of the interface region the 50S and 60S subunits are very similar, while in regions more distant from this surface they diverge.

In orthogonal rotations around the vertical axis the 60S subunit appears little different from the 50S subunit, notably in the kidney view seen when the subunits are in a side-by-side rotation of the ribosome (Fig. 1E and J).

Comparison with ribosomes from higher eukaryotes

This report characterizes the third medium resolution eukaryotic ribosome structure to be achieved by cryo electron microscopic methods, after the wheatgerm (3) and rabbit (40S subunit only; 24) ribosomes. In comparing the constituents of these three ribosomes we note that the yeast and plant rRNAs are quite similar in size, while the mammalian rRNAs are larger, by ~10% for the 40S subunit and by nearly 33% for the 60S subunit (26). The current catalog of ribosomal proteins is probably complete for yeast and mammals. The latter have only a single additional protein, although many mammalian ribosomal proteins are slightly larger than their yeast homologs. While we as yet lack sufficient data to fully evaluate the plant ribosomal proteins, there is no reason to believe, from the data described thus far, that they will be appreciably different.

The principal difference between the two 80S ribosome structures, wheatgerm and yeast, is a difference in proportions. Relative to the wheatgerm structure, the yeast ribosome appears more compact in height and width (Fig. 2C) and notably more globular. It is also greater in thickness (see below). Compared with the wheatgerm structure, resolution into two separate subunits is superior for the yeast structure in the lower or body portion of the ribosome. Except for the central bridge and the bridge between the bases, the two subunits are completely distinct, at least at the threshold used in this study.

The notable difference in thickness between the yeast and wheatgerm structures points up a cautionary note. Several differences in methods exist between the studies, which make a strict comparison problematical. The wheatgerm data had a missing cone of angular information, due to the random conical tilt geometry used, which was compensated for by the use of POCS techniques (see for example 11). In the yeast study, however, angular space was completely (albeit unevenly) infilled and POCS was not applied. Moreover, a different back-projection algorithm was used, in which a constraint similar to one of the POCS constraints was in effect. As well as this difference in data collection geometry and computational techniques between the studies, one preparational difference cannot be excluded as having some bearing on the comparison. The yeast ribosomes were high salt washed, in order to ensure that non-ribosomal components were not present. This could possibly give rise to an enhanced openness of the upper intersubunit space. However, the ability to visually separate the subunits is probably due more to higher effective resolution (due to the far larger number of projections in the image data set used for reconstruction) than to stripping off of factors and ligands.

One final comparison with a 40S ribosome structure from rabbit reticulocytes (24) is surprising. The yeast small subunit structure in both frontal and lateral views more strongly resembles this mammalian 40S subunit structure than it does the wheatgerm 40S structure. (Intermediate views of the rabbit structure were compromised by loss of information in certain angular ranges due to the missing cone.) Particularly for the crest, beak, enrolled front lobe (23), cupped platform and pointed front foot the agreement is unexpectedly good. Why the details of the morphology of the yeast 40S subunit should resemble those seen for a mammalian subunit (which has a slightly larger 18S RNA) more closely than those seen for a higher plant (with an 18S RNA very similar in size to that of yeast) is unclear. The data collection and methods of analysis of the two earlier structures, rabbit and wheatgerm, were closely similar to one another, whereas the methods for yeast ribosome analysis were in some respects closer to the methods used for the *E.coli* reconstructions (where data from a larger angular range could be used; see for example 18,19).

Internal structure of the yeast ribosome: the exit tunnel

Since completion of the reconstruction reported here recent continued studies at improving resolution on the *E.coli* and yeast ribosomes (21; Malhotra *et al.*, submitted for publication; Verschoor *et al.*, work in progress) have led to the consistent finding of a low density 'tunnel' feature extending from the IC to the lower back of the large subunit. Although other prominent low density features can be discerned in individual reconstructions, the siting and orientation of what is apparently a conserved feature is of primary interest.

Although we are interested in eukaryotic specializations related to, for example, membrane attachment, we must first identify features related to the most universal functions in the translation process. If we accept the experimental evidence that a tunnel traverses the large ribosomal subunit for the purpose of conducting the nascent chain from the peptidyltransferase center (PTC) then we should be able to identify this tunnel feature in eubacteria, Archaea and eukaryotes. The existence of such a tunnel through the large subunit is strongly implied by studies involving iodide ion quenching of nascent chain photoreactive probes (see for example 27), in which the nascent chain is shown not to be exposed to the cytoplasm in membrane-bound ribosomes.

It is surprising, at the moderate resolution of this study, that a feature as small as the exit hole should be so distinct. The 60S subunit can be sighted through from the IC side (Fig. 2A) to the back (Fig. 2) at an only slightly elevated threshold. There is a clear qualitative difference between this unique feature and the larger, smooth holes or cavities that appear as the structure pinches out in thin regions once a locally critical threshold is reached. Internally the effects of resolution limitation can be seen in the fact that the goblet structure, although open to and in communication with the IC, retracts away from it to form the wavy rim feature.

At higher resolution in both *E.coli* (18, Figs 3 and 4 ; 19, Fig. 2) and yeast (21; Verschoor *et al.*, work in progress) the tunnel is seen to be more tubular, i.e. less variable in width than the rapid taper seen in the present yeast structure. However, not only is the trend of the feature identical, but the siting of the exit hole on the lower back of the large subunit also corresponds precisely. This hole has subsequently been demonstrated to be involved in post-translational processing of the nascent chain. In a study just completed on a 3D reconstruction of the yeast sec61p–ribosome complex (21) the central pore of the sec61p complex, which is involved in signal sequence recognition and binds directly to the ribosome, aligns precisely with the hole marking the debouchement of this tunnel feature, suggesting that the nascent chain is conducted successively through tunnel and pore after its formation at the PTC.

Thus we are able to use the strong structural conservation of the ribosome to delineate internal features that are strikingly alike in ribosomes from different taxa. Ligand experiments such as the one just described can then confirm that these well-characterized morphological features interact with ligands of known function, which demonstrates that we are indeed justified in assigning functional roles to such features.

CONCLUSIONS

The structure calculated for the yeast ribosome leaves no question that the architecture of the translational machinery of the cell has been strongly conserved from one kingdom to another. The degree of resemblance to the eubacterial (*E.coli*) ribosome is considerable, while the similarity of this lower eukaryotic ribosome to the ribosome of a higher eukaryote (wheatgerm) is also unambiguous. Thus the task of tracing fundamental translational processes, such as the itineraries of the mRNA and tRNAs into and out of the ribosome, is to some degree simplified if we are able to recognize the same structural landmarks on evolutionarily divergent ribosomes and to understand how they delineate functional domains that are strongly conserved. Then, conversely, we can also identify *non*-conserved features and begin to explore their possible functions in terms of known inter-kingdom differences or variations in the translational process.

The data presented above will serve as a baseline for future studies. *Saccharomyces cerevisiae* is perhaps the one eukaryote for which we have both the genetic data and the genetic tools to approach a structure–function study of the ribosome. There are a number of yeast ribosomal proteins which are not essential for life yet which are important for optimal assembly, stability and function of the ribosome (28). In addition, there are mutant ribosomal proteins that have a substantial effect on the accuracy of the ribosome's translational capabilities (29). There exist more general mutations, such as those that block *N*-acetylation of numerous ribosomal proteins (30) without having much apparent effect on ribosome function. As cryo electron microscopy continues to advance it is likely to become the method of choice for understanding the subtle effects of mutations such as these and for reconciling the differences that inevitably appear between prokaryotic and eukaryotic ribosomes.

ACKNOWLEDGEMENTS

Financial support to J.F. from the NIH (1R01 GM 29169) and NSF (BIR 9219043) and to J.R.W. (NIH 1R01 GM 35532) is gratefully acknowledged. We thank Arun Malhotra, Pawel Penczek and Amy Heagle for assistance with visualization in the preparation of the final manuscript.

REFERENCES

1 Goffeau,A., Aert,R., Agostini-Carbone,M.L., *et al.* (1997) *Nature*, **387,** Suppl. to issue 6632.
2 Wool,I.G., Chan,Y.-L. and Gluck,A. (1996) In Hershey,J.W.B., Mathews,M.B. and Sonenberg,N. (eds), *Translational Control*. Cold Spring Harbor Laboratory Press, Cold Spring Harbor, NY, pp. 685–732.

3 Verschoor,A., Srivastava,S., Grassucci,R. and Frank,J. (1996) *J. Cell Biol.*, **133,** 495–505.
4 Thomas,B.J. and Rothstein,R. (1989) *Cell*, **56,** 619–630.
5 Warner,J.R. and Gorenstein,C. (1978) In Prescott,D. (ed.), *Methods in Cell Biology.* Academic Press, New York, NY, Vol. XX, pp. 45–60.
6 Chakravarti,D., Maiti,T. and Maitra,U. (1993) *J. Biol. Chem.*, **268**, 5754–5762.
7 Huang,H.-K., Yoon,H., Hannig,E.M. and Donahue,T.F. (1997) *Genes Dev.*, **11,** 2396–2413.
8 Wagenknecht,T., Grassucci,R. and Frank,J. (1988) *J. Mol. Biol.*, **199**, 137–145.
9 Dubochet,J., Adrian,M., Chang,J.-J., Homo,J.-C., Lepault,J., McDowall,A.W. and Schultz,P. (1988) *Q. Rev. Biophys.*, **21,** 129–132.
10 Penczek,P.A., Grassucci,R.A. and Frank,J. (1994) *Ultramicroscopy*, **53**, 251–270.
11 Sezan,M.I. (1992) *Ultramicroscopy*, **40**, 55–67.
12 Penczek,P., Radermacher,M. and Frank,J. (1992) *Ultramicroscopy*, **40**, 33–53.
13 Jones.T.A., Zhouy,J.Y., Cowan,S.W. and Kjeldgaard,M. (1991) *Acta Crystallogr.*, **A47**, 110–119.
14 Boettcher,B., Wynne,S.A. and Crowther,R.A. (1997) *Nature*, **386**, 88–91.
15 Unser,M., Trus,B.L. and Steven,A.C. (1987) *Ultramicroscopy*, **23**, 39–52.
16 Stark,H., Mueller,F., Orlova,E.V., Schatz,M., Dube,P., Erdemir,T., Zemlin,F., Brimacombe,R. and van Heel,M. (1995) *Structure*, **3,** 815–821.
17 Bielka,H. (ed.) (1982) *The Eukaryotic Ribosome.* Springer-Verlag, Berlin, Germany.
18 Frank,J., Zhu,J., Penczek,P., Li,Y., Srivastava,S., Verschoor,A., Radermacher,M., Grassucci,R., Lata,R.K. and Agrawal,R.K. (1995) *Nature*, **376**, 441–444.
19 Frank,J., Verschoor,A., Li,Y., Zhu,J., Lata,R.K., Radermacher,M., Penczek,P., Grassucci,R., Agrawal,R.K. and Srivastava,S. (1995) *Biochem. Cell Biol.*, **73**, 757–765.
20 Frank,J. and Agrawal,R.K. (1998) *Biophys. J.*, **74**, in press.
21 Beckman,R., Bubeck,D., Grassucci,R., Penczek,P., Verschoor,A. and Frank,J., (1987) *Science*, in press.
22 Verschoor,A., Zhang,N.-Y., Wagenknecht,T., Obrig,T., Radermacher,M. and Frank,J. (1989) *J. Mol. Biol.*, **209**, 115–126.
23 Verschoor,A. and Frank,J. (1990) *J. Mol. Biol.*, **214**, 737–749.
24 Srivastava,S., Verschoor,A., Radermacher,M., Grassucci,R. and Frank,J. (1995) *J. Mol. Biol.*, **245**, 461–466.
25 Frank,J., Verschoor,A. and Wagenknecht,T. (1985) In Wu,T.T. (ed.), *New Methodologies in Studies of Protein Configuration.* Van Nostrand Reinhold Co., New York, NY.
26 De Rijk,P., Van de Peer,Y. and De Wachter,R. (1996) *Nucleic Acids Res.*, **24**, 92–97.
27 Crowley,K.S., Reinhart,G.D. and Johnson,A.E. (1993) *Cell*, **73**, 1101–1115.
28 Baronas-Lowell,D.M. and Warner,J.R. (1990) *Mol. Cell. Biol.*, **10**, 5235–5243.
29 Alksne,L.E., Anthony,R.A., Liebman,S.W. and Warner,J.R. (1993) *Proc. Natl. Acad. Sci. USA*, **90**, 9538–9541.
30 Takakura,H., Tsunasawa,S., Miyagi,M. and Warner,J.R. (1992) *J. Biol. Chem.*, **267**, 5442–5445.